Neurocrit Care
https://doi.org/10.1007/s12028-020-00971-x

NEUROCRITICAL CARE SOCIETY

ORIGINAL WORK

Resting-State NIRS–EEG in Unresponsive Patients with Acute Brain Injury: A Proof-of-Concept Study

Marwan H. Othman[1†], Mahasweta Bhattacharya[2†], Kirsten Møller[3,4], Søren Kjeldsen[5], Johannes Grand[5], Jesper Kjaergaard[4,5], Anirban Dutta[2] and Daniel Kondziella[1,4*]

Abstract

Background: Neurovascular-based imaging techniques such as functional MRI (fMRI) may reveal signs of consciousness in clinically unresponsive patients but are often subject to logistical challenges in the intensive care unit (ICU). Near-infrared spectroscopy (NIRS) is another neurovascular imaging technique but low cost, can be performed serially at the bedside, and may be combined with electroencephalography (EEG), which are important advantages compared to fMRI. Combined NIRS–EEG, however, has never been evaluated for the assessment of neurovascular coupling and consciousness in acute brain injury.

Methods: We explored resting-state oscillations in eight-channel NIRS oxyhemoglobin and eight-channel EEG band-power signals to assess neurovascular coupling, the prerequisite for neurovascular-based imaging detection of consciousness, in patients with acute brain injury in the ICU ($n = 9$). Conscious neurological patients from step-down units and wards served as controls ($n = 14$). Unsupervised adaptive mixture-independent component analysis (AMICA) was used to correlate NIRS–EEG data with levels of consciousness and clinical outcome.

Results: Neurovascular coupling between NIRS oxyhemoglobin (0.07–0.13 Hz) and EEG band-power (1–12 Hz) signals at frontal areas was sensitive and prognostic to changing consciousness levels. AMICA revealed a mixture of five models from EEG data, with the relative probabilities of these models reflecting levels of consciousness over multiple days, although the accuracy was less than 85%. However, when combined with two channels of bilateral frontal neurovascular coupling, weighted *k*-nearest neighbor classification of AMICA probabilities distinguished unresponsive patients from conscious controls with > 90% accuracy (positive predictive value 93%, false discovery rate 7%) and, additionally, identified patients who subsequently failed to recover consciousness with > 99% accuracy.

Discussion: We suggest that NIRS–EEG for monitoring of acute brain injury in the ICU is worthy of further exploration. Normalization of neurovascular coupling may herald recovery of consciousness after acute brain injury.

Keywords: Cardiac arrest, Coma, Consciousness, Electroencephalography, Near-infrared spectroscopy, Neurovascular coupling, Neurovascular unit, Prognosis, Traumatic brain injury

*Correspondence: daniel_kondziella@yahoo.com
†Marwan H. Othman and Mahasweta Bhattacharya have contributed equally to this work.
‡Anirban Dutta and Daniel Kondziella have contributed equally to this work.
[1] Department of Neurology, Rigshospitalet, Copenhagen University Hospital, Blegdamsvej 9, 2100 Copenhagen, Denmark
Full list of author information is available at the end of the article

Introduction

Neurovascular coupling refers to interactions within the "neurovascular unit," which consists of neurons, astrocytes, and vascular cells, including the blood–brain barrier (Fig. 1). Briefly, neuronal activation is accompanied by increased cerebral blood flow and

Springer

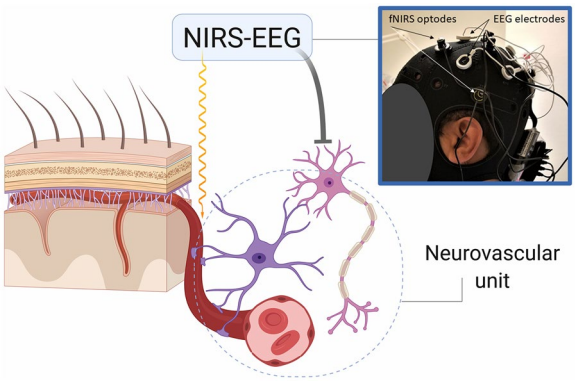

Fig. 1 Resting-state NIRS-EEG, using a wireless wearable bedside device, allows evaluation of the neurovascular unit, consisting of astrocytes and other glial cells, neurons, and blood vessel cells. Neuronal (EEG) and hemodynamic (NIRS) signals are characterized by a dominant frequency at 0.1 Hz [34]. We postulated that NIRS oxy-hemoglobin oscillations between 0.07 and 0.13 Hz would be found in most acute brain injury patients, but that the state of the neurovascular coupling would be affected by the level of consciousness, and that recovery of neurovascular coupling would occur in parallel with recovery of consciousness. EEG—electroencephalography; fNIRS—functional near-infrared spectroscopy

increased cerebral metabolic rate for oxygen, leading to functional hyperemia and energy supply [1]. Neurovascular coupling thus reflects the close temporal and regional connection between neuronal activity and cerebral blood flow [1–4]. Functional brain imaging techniques such as functional magnetic resonance imaging (fMRI) and near-infrared spectroscopy (NIRS) rely on neurovascular coupling to infer changes in neuronal activity; and neurovascular coupling is the basis of the BOLD fMRI signal. Of note, some brain-injured patients who are unresponsive at the bedside show evidence of (partially) preserved consciousness when examined by active and/or resting-state fMRI [5–10]. However, fMRI-based paradigms are labor intensive, expensive, logistically challenging, and not readily available in the intensive care unit (ICU) [9–11]. A cheap, easy-to-apply test for consciousness assessment is needed.

NIRS and EEG are low-cost devices that can be administered at the bedside, which is an important advantage in the ICU compared to fMRI [12]. EEG captures neuronal activities with poor spatial (centimeters) but excellent temporal (milliseconds) resolution. EEG within 24 h predicts neurological outcome of comatose patients after cardiac arrest, albeit with low sensitivity [13, 14]. Since altered hemodynamics contributes to anoxic damage, integrating neurovascular coupling in the assessment of patients with anoxic brain injury might help to increase sensitivity [15].

NIRS is a promising tool in this regard. A noninvasive optical method, NIRS measures local changes in oxygenated and deoxygenated hemoglobin in the outmost layers of the cerebral cortex, consistent with spontaneous cerebral oscillations [16–23]. Low (≈0.1 Hz) and very low (≈0.05 to 0.01 Hz) frequency oscillations of oxy-Hb are believed to reflect cortical cerebral autoregulation. Thus, like transcranial Doppler, NIRS assesses cerebral autoregulation with high temporal resolution, but while Doppler measures blood flow velocity in large cerebral vessels, NIRS detects changes in microcirculatory blood volume and blood flow by measuring cortical oxy-Hb and deoxy-Hb. NIRS offers distinct advantages compared to transcranial Doppler in being operator independent, easier to perform and assessing cortical tissue. Methodologies based on NIRS have been applied in a variety of neurological conditions, including ischemic stroke [e.g., 18,24,26–28], subarachnoid hemorrhage [27], migraine [23], traumatic brain injury [28], post-cardiac arrest anoxic brain injury [29], and neonatal encephalopathy [15, 30]. For a recent review about the application of NIRS in neurological conditions, including technical and analytical limitations, see [31]. NIRS captures cerebral metabolic changes with lower temporal resolution than EEG because of the inherent hemodynamic delay, but NIRS has better spatial resolution and is less susceptible to electrical noise, sedation and muscle artifacts [12, 25, 28]. (Commercially available portable functional NIRS systems have a depth sensitivity of about 1.5 cm and a spatial resolution up to 1 cm [32].) Functional imaging signals are characterized by slow fluctuations (≤0.1 Hz) [33], originating from neuronal (EEG) and, as already explained, hemodynamic (NIRS) signals [34], which have been proposed as "central pacemaker oscillations" [35]. The vascular origin of these 0.1 Hz oscillations has been assigned to vasomotion [36] and Mayer waves [37], and the neuronal origin to neurovascular coupling [38–40].

While EEG and fMRI have long-standing roles for the evaluation of consciousness following brain injury [8], the application of NIRS in this field has recently gained momentum [4, 41–45]. Of note, NIRS–EEG hybrid systems combine the benefits from EEG and NIRS (Fig. 1), while avoiding the logistical challenges associated with fMRI. Neurovascular coupling revealed by NIRS–EEG has been proposed as an important feature of the resting brain, the hypothesis being that the aforementioned fluctuations of EEG band-power corresponding with the NIRS oxyhemoglobin oscillations around 0.1 Hz represent fluctuations in brain excitability [26, 38, 40]. Corroborating this idea, cerebral excitability is more impaired in the vegetative state/unresponsive wakefulness syndrome (VS/UWS) than in the minimally conscious state (MCS) [46]. However, although NIRS–EEG has been studied in

(See figure on next page.)

Fig. 2 This figure depicts methods of signal processing and statistical analysis used in the present study, which can be divided into three components (**a**–**c**). Continuous and non-stationary (i.e., constantly fluctuating) dynamics of brain network activity, underlying human cognition and behavior, are challenging to assess by statistical evaluation, but adaptive mixture-independent component analysis (AMICA) may be a suitable approach [52] (**a**, blue). AMICA performs an independent component analysis decomposition on EEG data with five ICA models to model EEG dynamics that are associated with brain state changes during the recovery of consciousness. AMICA consists of three layers of mixing, where the first layer consists of mixture of ICA models that learn the underlying data clusters, the second layer consists of mixture of independent components (ICs) that decompose the data cluster into statistically independent source activations, and the third layer consists of mixture of generalized Gaussian distribution that approximates the probability distribution of the source activation. Non-stationary model probabilities of the five ICA models that were learned by AMICA EEG decomposition were used in conjunction with the averaged wavelet coherence (**b**, yellow) between the NIRS oxygenated hemoglobin signal in the frequency band between 0.07 Hz and 0.13 Hz and the EEG band-power (1–12 Hz) signal at the frontal areas (F3 and F4, 10–20 system) as features for classification of unresponsive/low-responsive patients from conscious controls as well as prognostication of consciousness recovery. Here, the first two principal components of the non-stationary model probabilities of the five ICA models accounted for > 90% variance, which along with two channels of averaged wavelet coherence were used in the weighted *k*-nearest ($k = 10$, Euclidean distance metric with squared inverse distance weight) neighbor classifier and evaluated based on receiver operating characteristic curve (**c**, green). AMICA—adaptive mixture-independent component analysis; EEG—electroencephalography; fNIRS—functional near-infrared spectroscopy; ICs—independent components; PDFs—probability density functions (Color figure online)

children with perinatal hypoxic injury [47–50], it has not yet been applied to adults with acute brain injury.

In the present study, we explored the feasibility of low-density NIRS–EEG to assess the evolution of neurovascular coupling with improving (or declining) levels of consciousness in unresponsive adult patients with acute brain injury. We postulated that resting-state frontal NIRS oxyhemoglobin oscillations would be increasingly coupled with EEG band-power oscillations [38], when consciousness recovers after brain injury, reflecting increased cerebral excitability.

Primary objective: To assess the feasibility of NIRS–EEG for the assessment of neurovascular coupling and the classification of consciousness levels in ICU patients with brain injury

We hypothesized that neurovascular coupling in patients from the ICU and step-down units could be evaluated with low-density (eight-channel) resting-state NIRS-EEG. We further hypothesized that an adaptive mixture-independent component analysis (AMICA) [51] classifier could be trained to learn the transiently changing models across different levels of consciousness, thereby assessing neurovascular coupling during deterioration and recovery of consciousness [52] (Fig. 2). Such a probabilistic mixture framework enables accommodation of non-stationary environments and arbitrary EEG source densities [53] which occur with shifting consciousness levels in physiological [54] and unphysiological conditions [48, 49].

Secondary objective: To assess the feasibility of NIRS–EEG for prognostication of ICU patients with brain injury following cardiac arrest or trauma

We finally hypothesized that neurovascular coupling data from NIRS–EEG would enable us to distinguish patients who recover consciousness from those who fail to do so. Hence, we expected patients with good prognosis to show rapid normalization of neurovascular coupling after cessation of sedation, while this would not be the case in patients with poor prognosis.

Methods

Target Population, Inclusion and Exclusion Criteria, and Clinical Investigations

NIRS–EEG assessments were performed in a convenience sample of neurological/neurosurgical patients in the neuro-ICU and post-cardiac arrest patients in the cardiological ICU at a tertiary referral hospital ($n = 9$). Exclusion criteria were major scalp injury and acute life-threatening cardiovascular instability. Conscious patients, admitted to the neurological step-down unit, served as controls ($n = 14$). Levels of consciousness were estimated by MHO under the supervision of DK, a board-certified neurologist experienced in neurocritical care, following detailed neurological examination, including the Full Outline of UnResponsiveness (FOUR) [55], and categorized into coma, VS/UWS, minimal conscious state (MCS) minus, MCS plus, or emerged from MCS (eMCS) [56–58]. Briefly, coma was defined as a state of profound unawareness from which patients cannot be aroused, while eyes are closed, and a normal sleep–wake cycle is absent [59]. We diagnosed VS/UWS, if patients opened their eyes but exhibited only reflex behaviors and were considered unaware of themselves and their surroundings [60]. Further, we classified patients as MCS, when they showed unequivocal signs of non-reflex behaviors occurring inconsistently, yet reproducibly, in response to environmental stimuli [61]. MCS patients were further classified into MCS plus (i.e., if they were able to obey commands) or MCS minus (i.e., if they localized pain, exhibited visual pursuit, or showed appropriate emotional expressions) [62]. Patients who recovered functional communication

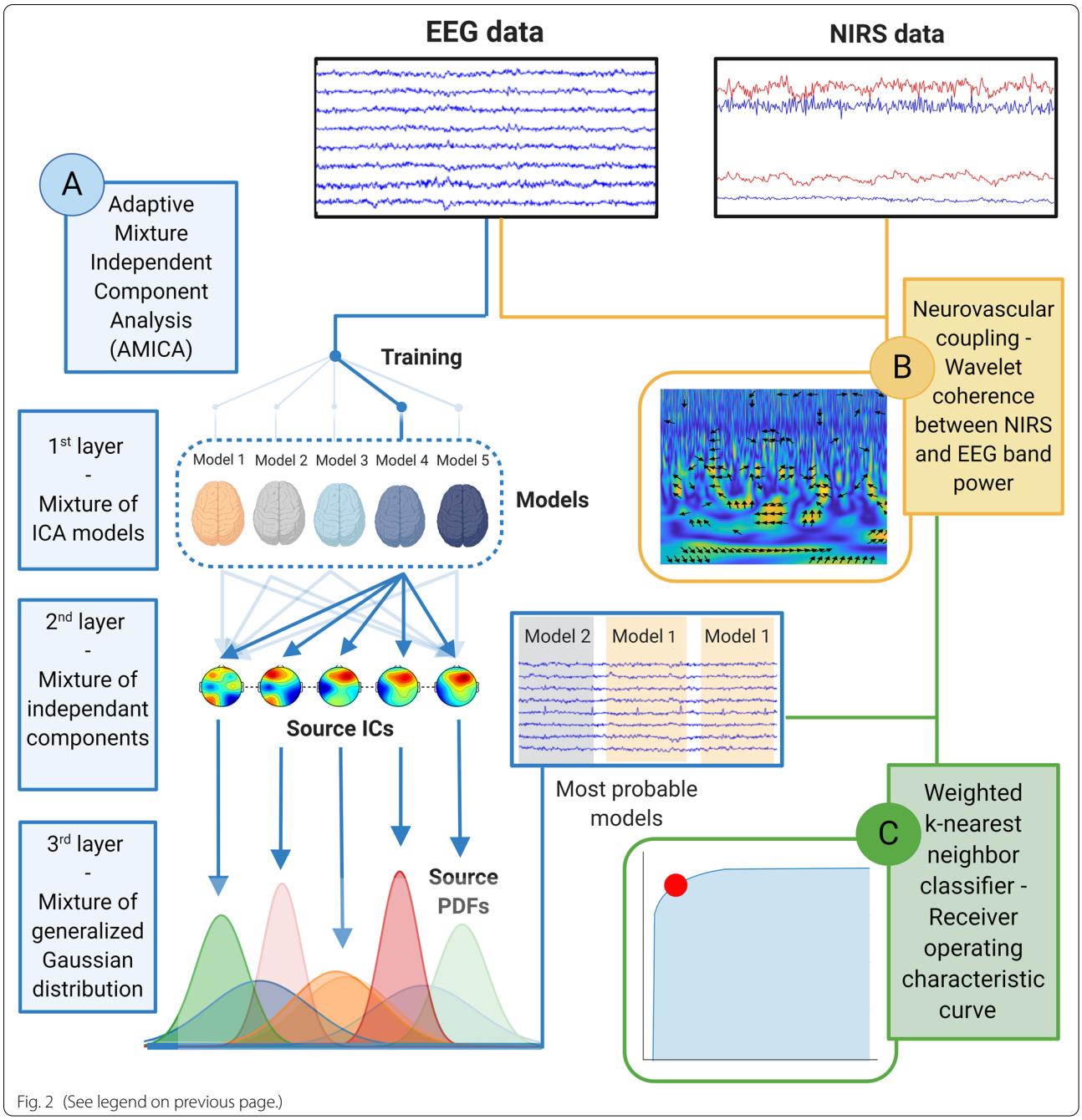

Fig. 2 (See legend on previous page.)

or functional object use were considered as "emerged from MCS" (eMCS) [61]. Hence, rather than the total FOUR score, classification of consciousness levels into coma, VS/UWS, MCS minus/plus, and eMCS was based on visual and motor FOUR subscales, as well as evidence of command following, appropriate emotional expressions, communication, and functional object use. Clinical data were stored in a dedicated database, following approval from local authorities.

Experimental Setup for NIRS–EEG Recordings

NIRS–EEG was conducted at the bedside, using the wireless StarStim NIRS–EEG system (Artinis Medical Systems, 6662 PW Elst, The Netherlands) [63] (*online supplemental files,* Figures S1 and S2). Technical details of the StarStim NIRS–EEG system [63] are as follows: for NIRS, eight source wavelengths at nominal 760 and 850 nm; two photodiodes with integrated ambient light protection; Bluetooth connection (up to 100 meters) for

online measurements at 50 Hz sampling rate; and up to 6 h of recording with one interchangeable and rechargeable battery. For EEG, 8 channels available at a sampling rate of 500 Hz; bandwidth: 0 to 125 Hz (DC coupled); resolution: 24 bits–0.05 μV resolution; noise: < 1 μV RMS; common mode rejection ratio: -115 dB; input impedance: 1 GΩ; and operating time: 5 h 10 min when using Wi-Fi connection. EEG data were processed using EEGLAB toolbox [64] in MATLAB.

We recorded from F3, F4, C3, C4, P3, and P4 scalp locations (10–20 positioning system) following Lehembre et al. [65] and added Fp1 and Fp2 scalp locations (10–20 positioning system) for prefrontal recordings. Eight NIRS sources were positioned at AF7, AF3, AF8, AF4, CP4, FC4, CP3, and FC3, and the two NIRS detectors at Cz and FPz at an optode distance of around 35 mm. The sensitivity analysis for the NIRS is explained in detail in the *online supplemental files* (Appendix). NIRS–EEG data [24] were recorded in 15-min segments for 45 min to 1 h with the patients resting and eyes closed. Unconscious patients were examined by resting-state NIRS–EEG from day 1 after admission to discharge from the ICU/step-down units.

AMICA Signal Processing, Neurovascular Coupling, and Classifier Training

Figure 2 provides an overview of data acquisition, signal processing and statistical analysis. Technical details are outlined (Appendix, *online supplemental files*). An independent statistical review of the methods, required by one of the referees of this paper, can be accessed online (Statistical Report, *online supplemental files*).

EEG data were first down-sampled to 250 Hz, following application of a 1–40 Hz band-pass filter, and the EEG data were then re-referenced to the common average. Then, the AMICA signal processing was applied (Appendix, *online supplemental files*). Briefly, AMICA is an unsupervised approach that can learn the models underlying non-stationary (i.e., constantly fluctuating) unlabeled EEG data (Fig. 2a). As outlined earlier, we postulated that AMICA models could capture the changing brain states that correspond to transitions between different levels of consciousness. Restated, AMICA may offer a promising unsupervised tool to learn the changes in EEG patterns, including those from low-density EEG recordings [52], during recovery of consciousness. As we aimed to categorize levels of consciousness into coma, VS/UWS, MCS minus, MCS plus and eMCS, five AMICA models were used with one model for each level of consciousness.

One of the challenges with NIRS data is a high sensitivity for scalp and other extracranial hemodynamics, including changes in the heartbeat and breathing cycle, which can mask cerebral activation [66]. Different methods have been proposed to remove extracranial hemodynamics from continuous-wave NIRS signal [67], including short-distance detector approaches [68] and tomography [69]. Thus, larger changes are observed in the extracranial oxygenated hemoglobin when compared to extracranial deoxygenated hemoglobin concentration. We used HOMER2 routines [70] in MATLAB (MathWorks, Inc.) for the NIRS data analysis based on the modified Beer–Lambert law (technical details in the Appendix, *online supplemental files*). We evaluated neurovascular coupling between NIRS oxygenated hemoglobin in the frequency band between 0.07 and 0.13 Hz and the EEG band-power (1-12 Hz) signals at the frontal areas (F3 and F4, 10–20 system), using wavelet cross-spectrum analysis (Fig. 2b). To determine the threshold for neurovascular coupling, we used the statistical test developed by Bigot and colleagues [71]. Thus, the wavelet coherence data between 0.07 and 0.13 Hz were divided into 1-min epochs ($N = 30$ for 30-min data) to measure statistical significance at alpha = 0.01 based on Bigot et al. [71]. For significant neurovascular coupling, the phase from the WCS was used to indicate the relative lag between NIRS oxygenated hemoglobin and the EEG band-power. A custom MATLAB script was written for these computations.

To illustrate the separability of NIRS–EEG data using the feature space learned by AMICA, we selected a weighted *k*-nearest neighbor classifier because of the low-dimensional data in our study (Fig. 2c). Rather than optimizing the classifier for the best performance, we wanted to prevent overfitting and to assess the generalization ability of our predictive model. So, we used a tenfold cross-validation, one of the most widely used data resampling methods [72], and computed confusion matrices and receiver operating characteristics curves (including area under the curves). The results were summarized for each weighted *k*-nearest neighbor classifier in the outcome measure.

Outcome Measures

Outcome measures include assessment of low-density NIRS–EEG data for the classification of the levels of consciousness (primary) and the prognostication of the recovery of the unresponsive patients with acute brain injury (secondary). These involved development of supervised classifier models using the Classification Learner app in the MATLAB (MathWorks, Inc.). We used AMICA model probabilities and neurovascular coupling as features and applied weighted *k*-nearest neighbor classification following principal component analysis (component reduction for 90% variance accounted for) to 2-s data windows to classify the NIRS–EEG data into (a)

unresponsive ICU patients with acute brain injury ($n=5$) versus 14 conscious controls; (b) 5 unresponsive ICU patients with acute brain injury into their FOUR scores—primary outcome measure; and (c) 5 unresponsive ICU patients with acute brain injury into those who regained consciousness ($n=3$) versus those who failed to recover ($n=2$)—secondary outcome measure. As said, due to low-dimensional data, weighted k-nearest neighbor classifier was used to illustrate the separability of NIRS–EEG data using the feature space learned by AMICA decomposition and neurovascular coupling. The tenfold cross-validation accuracy, confusion matrix, and the receiver operating characteristics curve were computed, and results were summarized for each weighted k-nearest neighbor classifier.

Ethics Statement

The Ethics Committee of the Capital Region of Denmark approved the study and waived the need for written consent because risks were deemed negligible (Reference J. No. H-19001774). The study was approved under the quality control legislation for commercially available medical devices, informed consent was waived, and data were anonymized prior to statistical analysis.

Results

Clinical Data

We enrolled a convenience sample of 23 patients (11 females; median age 63 years, range 19–79 years). From the ICU, we included patients who were monitored over multiple days ($n=5$) or only once ($n=4$). Six patients were in coma or VS/UWS at initial assessment. Diagnoses included anoxic encephalopathy after cardiac arrest, traumatic brain injury, and delirium associated with Guillain–Barré syndrome. NIRS–EEG monitoring and assessment of consciousness levels were performed in unsedated patients or, whenever deemed safe by the treating physicians, during wake-up calls (for dosages and infusion rates of sedatives, see *online supplemental files*). Table 1 provides details.

Conscious neurological patients from the neurological step-down unit served as controls ($n=14$; FOUR score 16; 8 females; median age 51.5 years, range 19–78 years). Diagnoses included multiple sclerosis ($n=3$), ischemic stroke ($n=3$), epilepsy, central nervous system lymphoma, central nervous system vasculitis, non-infectious myelitis, autoimmune encephalitis, motor neuron disease, Guillain–Barré syndrome, and Susac syndrome (all $n=1$).

Cortical Sensitivity of the NIRS Montage

The PHOEBE approach [73] (technical details in Appendix, *online supplemental files*) validated optical scalp contact for all frontal optodes (sources at AF7, AF3, AF8, AF4, and detector at FPz) across 9 ICU subjects (one sample from Table 2 was discarded) and 14 controls from neurological step-down unit. However, the optodes at the central areas (sources CP4, FC4, CP3, FC3, and detector at Cz) were not consistent across most patients due to signal interference from the subjects' hair so were not analyzed.

Primary Study Objective: Classification of Consciousness Levels

In unresponsive or low-responsive (FOUR score ≤ 7) patients from the ICU, average EEG power at 11 Hz, 22 Hz, and 34 Hz (alpha and beta activity) was centered at right frontal areas, whereas average EEG power at 2 Hz (delta activity) and 6 Hz (theta activity) was centered at left frontal areas (Fig. 3a). Therefore, NIRS sources positioned at AF3 and AF4 and the NIRS detector at FPz were used for the two-channel neurovascular coupling data at bilateral frontal areas (F3 and F4, 10–20 system) to investigate recovery of neurovascular coupling based on WCS, as shown with an illustrative example in Figs. 3b. Representative examples of raw EEG data and raw NIRS data are provided in Figures S3 and S4; *online supplemental files*).

Multi-model AMICA (five models) processed at the Neuroscience Gateway [74] was completed in 15 h, 43 min. The temporal dynamics learned from the EEG data from ICU patients and conscious controls (in the neurological ward) with 30-s smoothing by the five-model AMICA showed that Models 1 and 2 were primarily active in conscious controls (class False), while models 2 and 3 were primarily active in unresponsive or low-responsive ICU patients (class True) with acute brain injury as shown in Fig. 4a. Models 4 and 5 were largely inactive in both patient groups. Figure 4b shows the differences in the recovery of neurovascular coupling in ICU patients based on the average wavelet coherence between 0.07 and 0.13 Hz at the frontal areas (F3 and F4, 10–20 system).

Separation of unconscious or low-responsive ICU patients from conscious controls: Principal component analysis of the temporal dynamics of the five-model AMICA from all ICU patients and conscious controls (in the neurological ward) showed that 100% variance was accounted for by four principal components with explained variance per component (in order): 79.6%, 15.2%, 4.0%, 1.2%, and 0%. Thus, the first two principal components accounted for > 90% variance, which along with two channels of neurovascular coupling data were used to develop weighted k-nearest neighbor classifier ($k=10$, Euclidean distance metric with squared inverse distance weight) to separate unresponsive or

Table 1 Patients recruited from intensive care units

Patient ID	Number of NIRS–EEG assessment	Age	Sex	Diagnosis	Days since admission	Intubated	Sedation[$]	FOUR score	Level of consciousness[&]
ICU 1	1.	79	M	Traumatic brain injury	4	Yes	No	5 (E0, M2, B2, R1)	Coma
	2.				5	Yes	No	11 (E4, M2, B4, R1)	MCS minus
	3.#				6	No	No	14 (E2, M4, B4, R4)	eMCS
	4.				7	No	No	14 (E2, M4, B4, R4)	eMCS
ICU 2	1.	55	F	Cardiac arrest	8	Yes	Propofol, remifentanil ‡ *	7 (E0, M2, B4, R1) ‡ 9 (E2, M2, B4, R1) *	VS/UWS
	2.				14	No	No	16 (E4, M4, B4, R4)	Conscious
ICU 3	1.	58	M	Cardiac arrest	3	Yes	No	4 (E0, M0, B4, R0)	Coma
	2.				4	Yes	No	4 (E0, M0, B4, R0)	Coma
	3.				7	Yes	No	4 (E0, M0, B4, R0)	Coma†
ICU 4	1.	60	M	Cardiac arrest	1	Yes	Propofol, fentanyl	4 (E0, M0, B4, R0)	Coma
	2.				2	Yes	Propofol, fentanyl*	13 (E4, M4, B4, R1) *	MCS plus
ICU 5	1.	59	F	Cardiac arrest	3	Yes	Remifentanil	3 (E0, M0, B2, R1)	Coma
	2.				4	Yes	Remifentanil	5 (E0, M0, B4, R1)	Coma
	3.				5	Yes	Remifentanil	7 (E1, M2, B4, R0)	VS/UWS
ICU 6	1.	65	M	Cardiac arrest	2	Yes	Propofol, fentanyl	2 (E0, M0, B2, R0)	Coma†
ICU 7	1.	63	M	Cardiac arrest	6	No	No	16 (E4, M4, B4, R4)	Conscious
ICU 8	1.	74	F	GBS, delirium	2	Yes	No	16 (E4, M4, B4, R4)	Conscious
ICU 9	1.	66	M	Cardiac arrest	2	Yes	Propofol, fentanyl*	16 (E4, M4, B4, R4) *	Conscious

See methods for information on conscious control patients ($n = 14$) recruited from a neurological step-down unit

eMCS—emerged from MCS, F—female, GBS—Guillain–Barré syndrome, ICU—intensive care unit, M—male, MCS—minimal conscious state, VS/UWS—vegetative state/unresponsive wakefulness syndrome

$ NIRS–EEG monitoring and assessment of consciousness levels were performed in unsedated patients or, whenever deemed safe by the treating physicians, during wake-up calls. Data on dosage and infusion rates of sedatives are provided in the *online supplemental files* (Table S2)

[&] Classification of consciousness levels was based on visual and motor FOUR subscales rather than the total score

[#] On day 6 after admission, this patient was extubated and transferred to the neurological step-down unit

[‡] Sedation was stopped during NIRS–EEG monitoring. FOUR score before wake-up call

[*] Sedation was stopped during NIRS–EEG monitoring. FOUR score after wake-up call

[†] Life-sustaining therapy was withdrawn 12–8 h after the last NIRS–EEG recording

low-responsive (FOUR score ≤ 14) ICU patients from conscious controls. The results of the confusion matrix from the tenfold cross-validation are tabulated in Table 2. This table also presents the area under the ROC curve to classify unresponsive or low-responsive (FOUR score ≤ 14) ICU patients. The classifier using NIRS–EEG data provided an accuracy of 91.4%; the positive predictive values and the false discovery rates for unresponsive or low-responsive (FOUR score ≤ 14) ICU patients being 93% and 7%, respectively, and 88% and 12% for conscious controls.

Classification of consciousness levels according to FOUR scores: Principal component analysis of the temporal dynamics of the five-model AMICA from ICU patients only showed that 100% variance was accounted for by four principal components with explained variance per component (in order): 35.7%, 32.4%, 22.8%, 9.1%, and 0%. Here, the first three principal components (accounting for $> 90\%$ variance) from the

Table 2 Correlation of EEG, respectively NIRS–EEG, data with levels of consciousness and clinical outcome

	True positive (%)	False positive (%)	Area under the curve
1a. KNN classifier to separate unresponsive patients (class True) in the ICU from conscious controls (EEG only)	82	15	0.89
1b. KNN classifier to separate unresponsive patients (class True) in the ICU from conscious controls (NIRS + EEG)	93	12	0.97
2a. KNN classifier to identify unresponsive patients in the ICU with recovery of consciousness (class True) versus those without (EEG only)	84	18	0.82
2b. KNN classifier to identify unresponsive patients in the ICU with recovery of consciousness (class True) versus those without (NIRS + EEG)	99	1	1

Performance of the weighted *k*-nearest neighbor classifier to classify in the ICU, 1. unresponsive patients (class True) and 2. unresponsive patients who recovered consciousness (class True), based on two principal components from the temporal dynamics of the five-model AMICA (EEG) data with or without two channels of neurovascular coupling (NIRS + EEG) data. See Methods and Results for details

ICU—intensive care unit, KNN—*k*-nearest neighbor classifier

temporal dynamics of the five-model AMICA along with two channels of neurovascular coupling data were used to develop weighted *k*-nearest neighbor classifier ($k = 10$, Euclidean distance metric with squared inverse distance weight) to identify the FOUR scores categorized as conscious, coma, VS/UWS, or MCS/eMCS of the ICU patients. The confusion matrix from the tenfold cross-validation is shown in Fig. 5a, and the ROC curve to classify fully conscious (FOUR = 16), coma, VS/UWS, and MCS/eMCS is shown in Fig. 5b. The accuracy was found to be 87.8%; the positive predictive values and the false discovery rates for the conscious, coma, VS/UWS, MCS/eMCS were 87% and 13%; 85% and 15%; 89% and 11%; and 93% and 7%, respectively. The ROC curves showed that the positive class, coma, VS/UWS, and MCS/eMCS could be classified with true positive rate greater than or equal to 90%; however, the fully conscious (FOUR = 16) state in the ICU patients (some under anesthesia) could be classified with true positive rate of 77% only.

Secondary Study Objective: Prognostication of Consciousness Recovery

To distinguish unresponsive ICU patients recovering consciousness from those failing to do so, we developed a weighted *k*-nearest neighbor classifier based on two principal components (> 90% variance accounted for) from the temporal dynamics of the five-model AMICA together with two channels of neurovascular coupling data from the first NIRS–EEG assessment of each patient. The results of the confusion matrix from the tenfold cross-validation are shown in Table 2. This table also presents the area under the ROC curve to identify patients who regained consciousness. The positive predictive value and the false discovery rate for unresponsive patients regaining consciousness were 99% and 1%, respectively, and 99% and 1% for those who failed to recover.

Discussion

Recovery of consciousness is a very important predictor for outcome after acute brain injury, and underestimation of consciousness levels in the ICU may cause premature treatment withdrawal [75]. Reliable assessment of consciousness levels after acute brain injury is highly desirable to better predict clinical outcome, to improve neurorehabilitation potential, and to decrease caregiver burden and health costs [8].

Integrity and activity of brain networks that are critical for the recovery of consciousness can be assessed using fMRI, but this is logistically challenging, expensive, and incompatible with prolonged monitoring. In contrast, NIRS, EEG, and NIRS–EEG are low-cost noninvasive neuromonitoring devices that can be performed serially or continuously at the bedside, without the need for in-hospital transport for imaging, which are important advantages in the ICU [12, 25, 28, 76–78]. Moreover, after correction for scalp and other extracranial hemodynamics [66], NIRS–EEG may provide an extra layer of information compared with EEG alone, because neurovascular coupling can be assessed. Neurovascular coupling is relatively unaffected by common anesthetics, including pentobarbital, isoflurane, and propofol [79]. Therefore, when compared to EEG alone, NIRS–EEG-based measures of the neurovascular coupling may provide a marker of the severity of brain injury with comparatively little influence from anesthetics [79].

In the present study, we showed the feasibility of applying a commercially available low-density NIRS–EEG bedside device to capture neurovascular coupling in unresponsive traumatic and non-traumatic patients with acute brain injury and conscious neurological inpatients (controls). We further showed the feasibility to train a

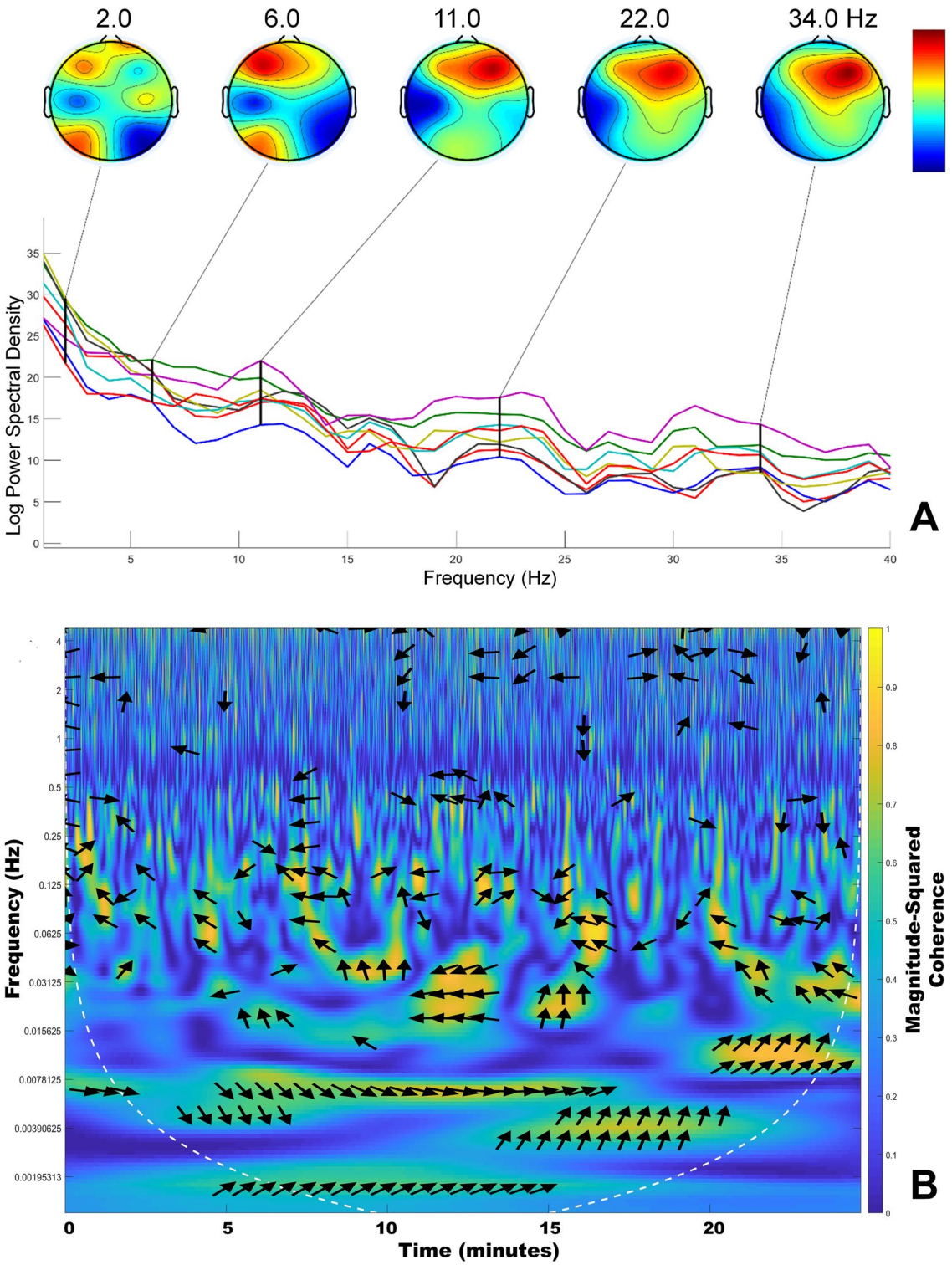

Fig. 3 **a** Topographical scalp map and power spectrum of the eight-channel EEG data at 2 Hz, 6 Hz, 11 Hz, 22 Hz, and 34 Hz from unresponsive patients in the ICU. **b** Neurovascular coupling was evaluated based on wavelet coherence between the NIRS O2Hb in the frequency band between 0.07 and 0.13 Hz and the EEG band-power (1–12 Hz) signals at the frontal areas (F3 and F4, 10–20 system). As an example, wavelet coherence between the NIRS O2Hb and the EEG band-power (1–12 Hz) signals is shown below for patient ICU 1, day 1 (at F3). For significant wavelet coherence, the phase lag of NIRS O2Hb with respect to EEG band-power (1–12 Hz) is shown with arrows that are spaced in time and scale. The direction of the arrows corresponds to the phase lag on the unit circle. Examples of raw EEG and raw NIRS data are provided in the *online supplemental files*

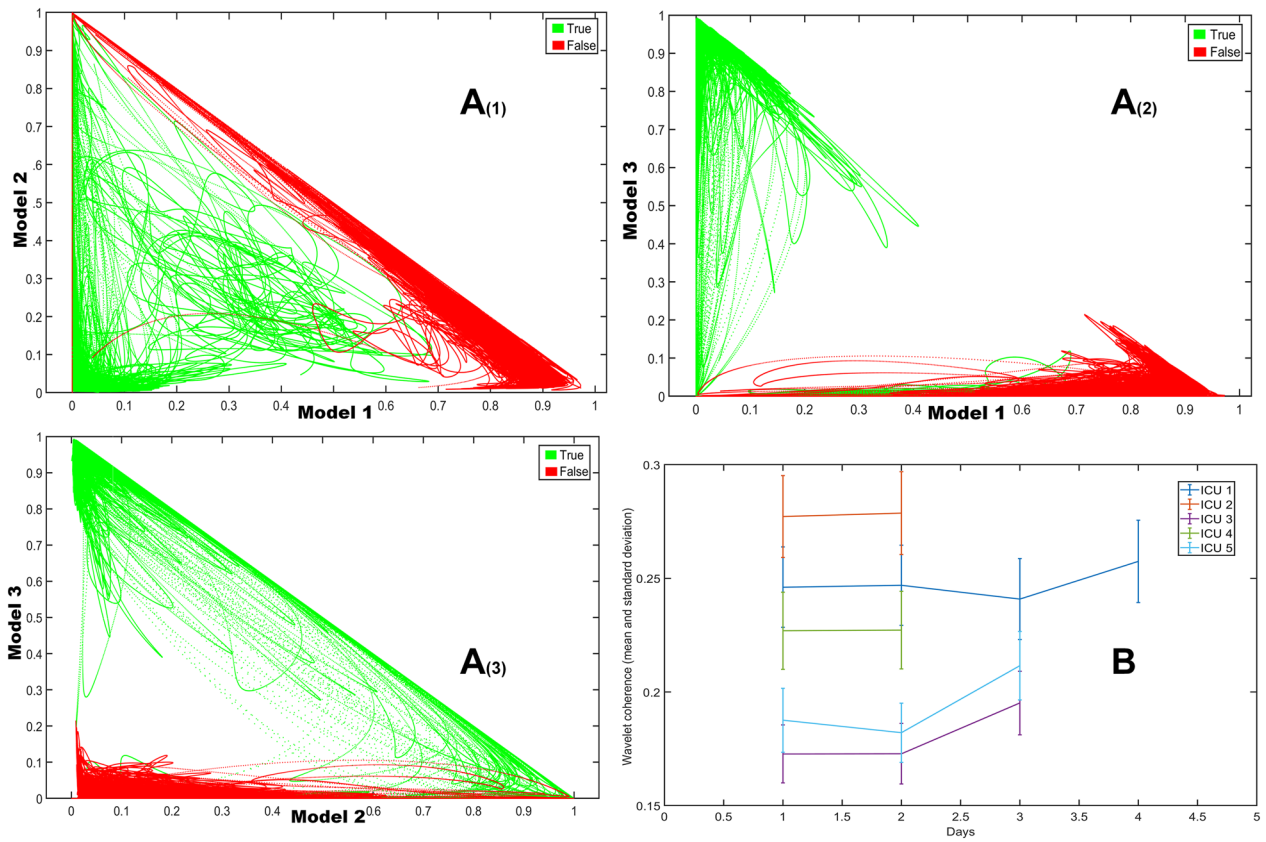

Fig. 4 **a** 1–3 Model probabilities of a five-model AMICA decomposition applied to the EEG recordings from unresponsive ICU patients (class True, green) and conscious controls (class False, red). Models 1 and 2 were primarily active in conscious controls, while models 2 and 3 were primarily active in unresponsive ICU patients with acute brain injury. **b** Differences in the recovery of neurovascular coupling in ICU patients (ICU 1–5, Table 1) were investigated based on the average wavelet coherence between 0.07 and 0.13 Hz at the frontal areas (F3 and F4, 10–20 system). Wavelet coherence above 0.14 was considered statistically significant for the averaged data over 30 epochs (total 30-min data)

machine learning algorithm to assess neurovascular coupling and potentially distinguish unresponsive patients from conscious controls (positive predictive value 93%), to classify the levels of consciousness after brain injury according to the FOUR score (positive predictive values between 85 and 93), and to differentiate unresponsive patients with recovery of consciousness from those without (positive predictive value 99%). (The accuracy was less than 85% when using the AMICA probabilities from EEG data only.)

It remains to be seen if NIRS–EEG performs differently in conditions of global brain injury (e.g., anoxia) compared to more focal injury (e.g., stroke, traumatic brain injury). From a clinical neuro-management perspective, the very limited spatial resolution of NIRS is an important limitation. Admittedly, NIRS shares this limitation with a range of other neuromonitoring devices that measure metabolism locally (albeit invasively) such as microdialysis [80, 81], brain temperature [82], and brain oxygen tension [82–85]. Documentation of neurovascular coupling in preserved brain tissue far remote from a brain lesion might be less helpful for prevention of secondary brain injury in the ICU. However, evidence of intact neurovascular coupling in crucial brain areas such as the frontal lobes might factor into algorithms for outcome prediction and classification of consciousness levels, as shown in the present study. In addition to resting-state NIRS–EEG, active NIRS paradigms based on, e.g., motor imagery to detect sign of preserved consciousness [41, 44, 86–90] might add a further layer of consciousness assessment in the ICU. Although active and resting-state fMRI paradigms have been shown to be feasible in the ICU [9, 10], NIRS–EEG would have an obvious advantage given the low costs and lack of major logistical challenges. Head-to-head studies comparing the diagnostic precision of fMRI to that of NIRS–EEG do not yet exist, to our knowledge.

This feasibility study has limitations that should be acknowledged. These include diagnostic heterogeneity, small numbers of subjects, and convenience sampling.

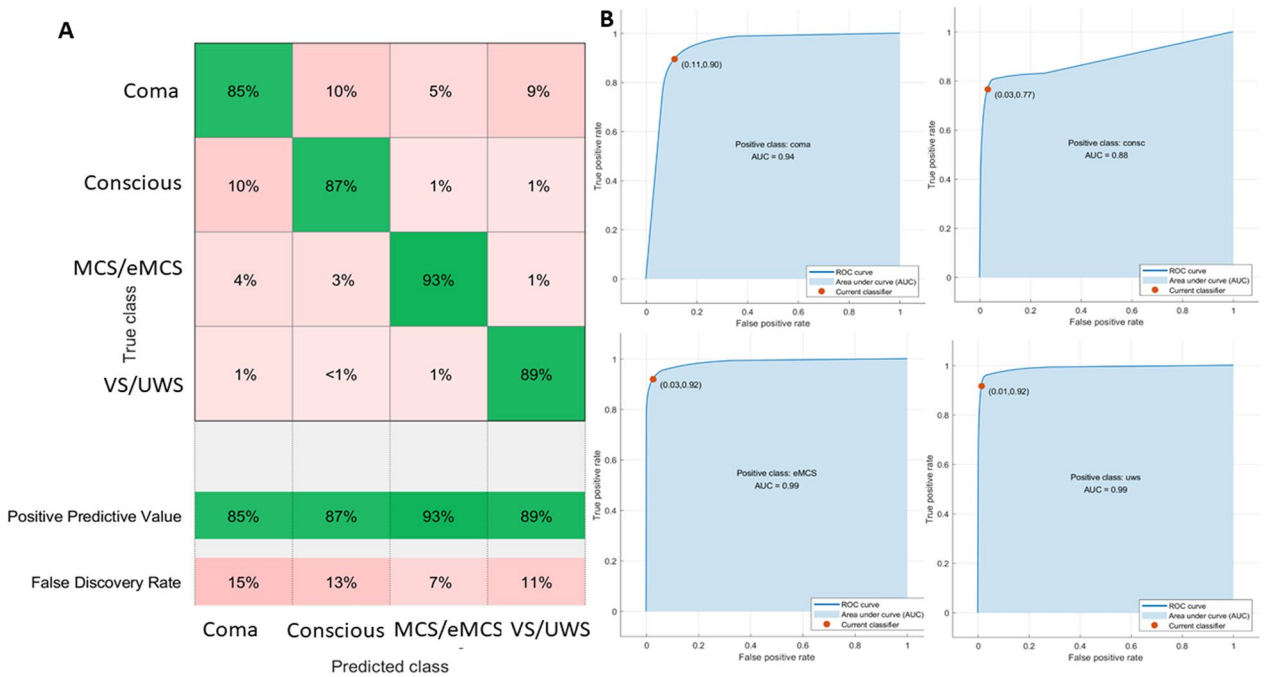

Fig. 5 **a** Confusion matrix for the weighted *k*-nearest neighbor (KNN) classifier to identify the FOUR scores categorized as coma, VS/UWS, minimal conscious state (MCS) minus, MCS plus, or emerged from MCS (eMCS) of unresponsive patients in the ICU (green, positive predictive values; pink, false predictive values). **b** Receiver operating characteristic curve for the weighted *k*-nearest neighbor classifier, based on two principal components from the temporal dynamics of the five-model AMICA together with two channels of neurovascular coupling data. AUC—area under the curve; ROC—receiver operating characteristics (Color figure online)

Most of our ICU patients had hypoxic-ischemic post-cardiac injury, which might not be generalizable to other neurocritical care settings. Moreover, some subjects were monitored for several days and some only once, if they were discharged or had life-supporting treatment withdrawn. Also, consciousness assessment was performed using neurological bedside examination, including the FOUR score, although the gold standard currently is the Coma Recovery Scale-Revised [91]. (Still, the FOUR is a reasonable alternative in ICU and more discriminative than the Glasgow Coma Scale [92, 93]). In addition, NIRS signal interference with the subjects' hair was noted for optodes at the central areas, which is an important technical limitation. Future studies with carefully controlled prospective patient enrollment and larger numbers will be needed to determine whether recovery of neurovascular coupling indeed signals recovery of consciousness, and whether low-density (i.e., 8 channels) is equal to or inferior to standard (e.g., 28 channels) or high-density (e.g., 256 channels) recordings. Finally, the present study was not powered to show that NIRS–EEG is undoubtedly associated with better algorithm performance than EEG alone, and this needs to be investigated further. On the positive side, strengths of the study include the true-to-life setting, careful avoidance of extracerebral NIRS signal contamination, and application of a tenfold cross-validation to prevent overfitting of our classifier. Further, an independent statistical review of the methods and statistics did not find cause for major concern (*online supplemental files*).

Conclusions and Future Directions

NIRS–EEG is a noninvasive, low-cost bedside device that allows serial evaluation of neurovascular coupling in a naturalistic ICU setting. The resulting data can be used to train a classifier to potentially distinguish unresponsive patients with good recovery from those without. Taken together, our results suggest that NIRS–EEG may be worth exploring in the future as an add-on to multimodal neuromonitoring. We hypothesize that recovery of neurovascular coupling after acute brain injury may herald recovery of consciousness. In the neurocritical care setting, this would be clinically meaningful information.

Electronic supplementary material

The online version of this article (https://doi.org/10.1007/s12028-020-00971-x) contains supplementary material, which is available to authorized users.

Author details
[1] Department of Neurology, Rigshospitalet, Copenhagen University Hospital, Blegdamsvej 9, 2100 Copenhagen, Denmark. [2] Department of Biomedical Engineering, University at Buffalo, State University of New York, Buffalo, NY, USA. [3] Department of Neuroanesthesiology, Copenhagen University Hospital, Copenhagen, Denmark. [4] Department of Clinical Medicine, Faculty of Health and Medical Sciences, University of Copenhagen, Copenhagen, Denmark. [5] Department of Cardiology, Rigshospitalet, Copenhagen University Hospital, Copenhagen, Denmark.

Author Contributions
AD, DK contributed to the study concept and design. MHO, KM, SK, JG, JK, AD, DK contributed to data acquisition. MB, AD, DK conducted data analysis and interpretation. AD, DK involved in writing of manuscript. MHO, MB, KM, SK, JG, JK, AD, DK provided important intellectual content.

Source of support
This work was supported by the Lundbeck Foundation (MW, DK), Offerfonden (DK), Savværksejer Jeppe Juhl og Hustru Ovita Juhls Mindelegat (DK), Region Hovedstadens Forskningsfond til Sundhedsforskning (DK), Jaschafonden (DK), Rigshospitalets Forskningspulje (DK), and NovoNordisk Foundation NNF17OC0028706 (JK, JG, and SK). AD and MB were supported by the University at Buffalo, USA. Figures 1 and 2 are created with biorender.com.

Conflict of interests
The authors declare no conflict of interests.

Ethical Approval/Informed Consent
The Ethics Committee of the Capital Region of Denmark approved the study and waived the need for written consent because risks were deemed negligible (Reference J. No. H-19001774).

Publisher's Note

Published online: 24 April 2020

References

1. Iadecola C. The neurovascular unit coming of age: a journey through neurovascular coupling in health and disease. Neuron. 2017;96:17–42.
2. Phillips AA, Chan FH, Zheng MMZ, Krassioukov AV, Ainslie PN. Neurovascular coupling in humans: physiology, methodological advances and clinical implications. J Cereb Blood Flow Metab. 2016;36:647–64.
3. Muoio V, Persson PB, Sendeski MM. The neurovascular unit—concept review. Acta Physiol. 2014;210:790–8.
4. Rupawala M, Dehghani H, Lucas SJE, Tino P, Cruse D. Shining a light on awareness: a review of functional near-infrared spectroscopy for prolonged disorders of consciousness. Front Neurol. 2018;9:350.
5. Owen AM, Coleman MR, Boly M, Davis MH, Laureys S, Pickard JD. Detecting awareness in the vegetative state. Science. 2006;313:1402.
6. Monti MM, Vanhaudenhuyse A, Coleman MR, Boly M, Pickard JD, Tshibanda L, et al. Willful modulation of brain activity in disorders of consciousness. N Engl J Med. 2010;362:579–89.
7. Stender J, Gosseries O, Bruno MA, Charland-Verville V, Vanhaudenhuyse A, Demertzi A, et al. Diagnostic precision of PET imaging and functional MRI in disorders of consciousness: a clinical validation study. Lancet. 2014;384:514–22.
8. Kondziella D, Friberg CK, Frokjaer VG, Fabricius M, Møller K. Preserved consciousness in vegetative and minimal conscious states: systematic review and meta-analysis. J Neurol Neurosurg Psychiatry. 2016;87:485–92.
9. Kondziella D, Fisher PM, Larsen VA, Hauerberg J, Fabricius M, Møller K, et al. Functional MRI for assessment of the default mode network in acute brain injury. Neurocrit Care. 2017;27:1–6.
10. Edlow BL, Chatelle C, Spencer CA, Chu CJ, Bodien YG, O'Connor KL, et al. Early detection of consciousness in patients with acute severe traumatic brain injury. Brain. 2017;140:2399–414.
11. Weijer C, Bruni T, Gofton T, Young GB, Norton L, Peterson A, et al. Ethical considerations in functional magnetic resonance imaging research in acutely comatose patients. Brain. 2016;139(Pt 1):292–9. https://doi.org/10.1093/brain/awv272.
12. Vinciguerra L, Bösel J. Noninvasive neuromonitoring: current utility in subarachnoid hemorrhage, traumatic brain injury, and stroke. Neurocrit Care. 2017;27:122–40.
13. Sondag L, Ruijter BJ, Tjepkema-Cloostermans MC, Beishuizen A, Bosch FH, van Til JA, et al. Early EEG for outcome prediction of postanoxic coma: Prospective cohort study with cost-minimization analysis. Crit Care. 2017;21(1):111.
14. Hofmeijer J, Beernink TMJ, Bosch FH, Beishuizen A, Tjepkema-Cloostermans MC, Van Putten MJAM. Early EEG contributes to multimodal outcome prediction of postanoxic coma. Neurology. 2015;85:137–43.
15. Chalak LF, Tian F, Adams-Huet B, Vasil D, Laptook A, Tarumi T, et al. Novel wavelet real time analysis of neurovascular coupling in neonatal encephalopathy. Sci Rep. 2017;7:45958.
16. Phillip D, Iversen HK, Schytz HW, Selb J, Boas DA, Ashina M. Altered low frequency oscillations of cortical vessels in patients with cerebrovascular occlusive disease—a NIRS study. Front Neurol. 2013;4:204.
17. Schytz HW, Guo S, Jensen LT, Kamar M, Nini A, Gress DR, et al. A new technology for detecting cerebral blood flow: a comparative study of ultrasound tagged NIRS and 133Xe-SPECT. Neurocrit Care. 2012;17:139–45.
18. Obrig H, Neufang M, Wenzel R, Kohl M, Steinbrink J, Einhäupl K, et al. Spontaneous low frequency oscillations of cerebral hemodynamics and metabolism in human adults. Neuroimage. 2000;12:623–39.
19. Haubrich C, Klemm A, Diehl RR, Möller-Hartmann W, Klötzsch C. M-wave analysis and passive tilt in patients with different degrees of carotid artery disease. Acta Neurol Scand. 2004;109:210–6.
20. Reinhard M, Wehrle-Wieland E, Grabiak D, Roth M, Guschlbauer B, Timmer J, et al. Oscillatory cerebral hemodynamics-the macro-versus microvascular level. J Neurol Sci. 2006;250:103–9.
21. Reinhard M, Schumacher FK, Rutsch S, Oeinck M, Timmer J, Mader I, et al. Spatial mapping of dynamic cerebral autoregulation by multichannel near-infrared spectroscopy in high-grade carotid artery disease. J Biomed Opt. 2014;19:097005.
22. Vernieri F, Tibuzzi F, Pasqualetti P, Rosato N, Passarelli F, Rossini PM, et al. Transcranial doppler and near-infrared spectroscopy can evaluate the hemodynamic effect of carotid artery occlusion. Stroke. 2004;35:64–70.
23. Schytz HW, Ciftçi K, Akin A, Ashina M, Bolay H. Intact neurovascular coupling during executive function in migraine without aura: interictal near-infrared spectroscopy study. Cephalalgia. 2010;30:457–66.
24. Guhathakurta D, Dutta A. Computational pipeline for NIRS–EEG joint imaging of tDCS-evoked cerebral responses-an application in ischemic stroke. Front Neurosci. 2016;10:261.
25. Hametner C, Stanarcevic P, Stampfl S, Rohde S, Veltkamp R, Bösel J. Noninvasive cerebral oximetry during endovascular therapy for acute ischemic stroke: an observational study. J Cereb Blood Flow Metab. 2015;35:1722–8.
26. Jindal U, Sood M, Chowdhury SR, Das A, Kondziella D, Dutta A. Corticospinal excitability changes to anodal tDCS elucidated with NIRS–EEG joint-imaging: an ischemic stroke study. In: 2015 37th Annual International Conference IEEE Engineering Medical Biology Society. IEEE; 2015. p. 3399–402. Available from: http://www.ncbi.nlm.nih.gov/pubmed/26737022.
27. Keller E, Froehlich J, Baumann D, Böcklin C, Sikorski C, Oberle M, et al. Detection of del ayed cerebral ischemia (DCI) in subarachnoid haemorrhage applying near-infrared spectroscopy: elimination of the extracerebral signal by transcutaneous and intraparenchymatous measurements in parallel. Acta Neurochir Suppl. 2015;120:243–7.
28. Zweifel C, Castellani G, Czosnyka M, Helmy A, Manktelow A, Carrera E, et al. Noninvasive monitoring of cerebrovascular reactivity with near infrared spectroscopy in head-injured patients. J Neurotrauma. 2010;27:1951–8.
29. Storm C, Leithner C, Krannich A, Wutzler A, Ploner CJ, Trenkmann L, et al. Regional cerebral oxygen saturation after cardiac arrest in 60 patients—a prospective outcome study. Resuscitation. 2014;85:1037–41.
30. Pichler G, Avian A, Binder C, Zotter H, Schmölzer GM, Morris N, et al. EEG and NIRS during transition and resuscitation after birth: Promising additional tools; an observational study. Resuscitation. 2013;84:974–8.

31. Andersen AV, Simonsen SA, Schytz HW, Iversen HK. Assessing low-frequency oscillations in cerebrovascular diseases and related conditions with near-infrared spectroscopy: a plausible method for evaluating cerebral autoregulation? Neurophotonics. 2018;5:1.
32. Ferrari M, Quaresima V. A brief review on the history of human functional near-infrared spectroscopy (fNIRS) development and fields of application. Neuroimage. 2012;63(2):921–35.
33. Mantini D, Perrucci MG, Del Gratta C, Romani GL, Corbetta M. Electrophysiological signatures of resting state networks in the human brain. Proc Natl Acad Sci USA. 2007;104:13170–5.
34. Pfurtscheller G, Schwerdtfeger A, Brunner C, Aigner C, Fink D, Brito J, et al. Distinction between neural and vascular BOLD oscillations and intertwined heart rate oscillations at 0.1 Hz in the resting state and during movement. PLoS One. 2017;12:0168097.
35. Pfurtscheller G, Schwerdtfeger AR, Seither-Preisler A, Brunner C, Stefan Aigner C, Brito J, et al. Brain–heart communication: evidence for "central pacemaker" oscillations with a dominant frequency at 0.1 Hz in the cingulum. Clin Neurophysiol. 2017;128:183–93.
36. Rayshubskiy A, Wojtasiewicz TJ, Mikell CB, Bouchard MB, Timerman D, Youngerman BE, et al. Direct, intraoperative observation of ~ 0.1 Hz hemodynamic oscillations in awake human cortex: implications for fMRI. Neuroimage. 2014;87:323–31.
37. Diehl RR, Linden D, Lücke D, Berlit P. Phase relationship between cerebral blood flow velocity and blood pressure. A clinical test of autoregulation. Stroke. 1995;26:1801–4.
38. Pfurtscheller G, Daly I, Bauernfeind G, Müller-Putz GR. Coupling between intrinsic prefrontal HbO2 and central EEG beta power oscillations in the resting brain. PLoS ONE. 2012;7:e43640.
39. Foster BL, Parvizi J. Resting oscillations and cross-frequency coupling in the human posteromedial cortex. Neuroimage. 2012;60:384–91.
40. Sood M, Besson P, Muthalib M, Jindal U, Perrey S, Dutta A, et al. NIRS–EEG joint imaging during transcranial direct current stimulation: Online parameter estimation with an autoregressive model. J Neurosci Methods. 2016;274:71–80.
41. Coyle SM, Ward TE, Markham CM. Brain-computer interface using a simplified functional near-infrared spectroscopy system. J Neural Eng. 2007;4:219–26.
42. Naseer N, Hong K-S. fNIRS-based brain-computer interfaces: a review. Front Hum Neurosci. 2015;9:3.
43. Holper L, Wolf M. Single-trial classification of motor imagery differing in task complexity: a functional near-infrared spectroscopy study. J Neuroeng Rehabil. 2011;8:34.
44. Koo B, Lee H-G, Nam Y, Kang H, Koh CS, Shin H-C, et al. A hybrid NIRS–EEG system for self-paced brain computer interface with online motor imagery. J Neurosci Methods. 2015;244:26–32.
45. Fu Y, Xiong X, Jiang C, Xu B, Li Y, Li H. Imagined hand clenching force and speed modulate brain activity and are classified by NIRS combined with EEG. IEEE Trans Neural Syst Rehabil Eng. 2017;25:1641–52.
46. Bai Y, Xia X, Kang J, Yang Y, He J, Li X. TDCS modulates cortical excitability in patients with disorders of consciousness. NeuroImage Clin. 2017;15:702–9.
47. Plomgaard AM, van Oeveren W, Petersen TH, Alderliesten T, Austin T, van Bel F, et al. The safeboosC II randomized trial: treatment guided by near-infrared spectroscopy reduces cerebral hypoxia without changing early biomarkers of brain injury. Pediatr Res. 2016;79:528–35.
48. Ancora G, Maranella E, Locatelli C, Pierantoni L, Faldella G. Changes in cerebral hemodynamics and amplitude integrated EEG in an asphyxiated newborn during and after cool cap treatment. Brain Dev. 2009;31:442–4.
49. Ancora G, Maranella E, Grandi S, Sbravati F, Coccolini E, Savini S, et al. Early predictors of short term neurodevelopmental outcome in asphyxiated cooled infants A combined brain amplitude integrated electroencephalography and near infrared spectroscopy study. Brain Dev. 2013;35:26–31.
50. Goeral K, Urlesberger B, Giordano V, Kasprian G, Wagner M, Schmidt L, et al. Prediction of outcome in neonates with hypoxic-ischemic encephalopathy II: role of amplitude-integrated electroencephalography and cerebral oxygen saturation measured by near-infrared spectroscopy Neonatology. 2017;112:193–202.
51. Palmer JA, Makeig S, Kreutz-Delgado K, Rao BD. Newton method for the ICA mixture model. In: IEEE international conference acoustics speech signal process. 2008. pp. 1805–8.
52. Hsu S-H, Pion-Tonachini L, Palmer J, Miyakoshi M, Makeig S, Jung T-P. Modeling brain dynamic state changes with adaptive mixture independent component analysis. Neuroimage. 2018;183:47–61.
53. Palmer JA, Kreutz-Delgado K, Makeig S. AMICA : an adaptive mixture of independent component analyzers with shared components. 2011.
54. Wu CW, Tsai P, Chen SC, Li C, Hsu A, Wu H, et al. Indication of dynamic neurovascular coupling from inconsistency between EEG and fMRI indices across sleep–wake states. Sleep Biol Rhythms. 2019;17:423–31.
55. Wijdicks EFM, Bamlet WR, Maramattom BV, Manno EM, McClelland RL. Validation of a new coma scale: The FOUR score. Ann Neurol. 2005;58:585–93.
56. Seel RT, Sherer M, Whyte J, Katz DI, Giacino JT, Rosenbaum AM, et al. Assessment scales for disorders of consciousness: Evidence-based recommendations for clinical practice and research. Arch Phys Med Rehabil. 2010;91(2):1795–813.
57. Giacino JT, Katz DI, Schiff ND, Whyte J, Ashman EJ, Ashwal S, et al. Comprehensive systematic review update summary: disorders of consciousness. Neurology. 2018. https://doi.org/10.1212/wnl.0000000000005928.
58. Trojano L, Moretta P, Masotta O, Loreto V, Estraneo A. Visual pursuit of one's own face in disorders of consciousness: a quantitative analysis. Brain Inj. 2018;32(2):1549–999.
59. Posner J, Plum F, Saper C. Plum and posner's diagnosis of stupor and coma. New York: Oxford University Press; 2007.
60. Laureys S, Celesia GG, Cohadon F, Lavrijsen J, León-Carrión J, Sannita WG, et al. Unresponsive wakefulness syndrome: a new name for the vegetative state or apallic syndrome. BMC Med. 2010;8:68.
61. Giacino JT, Ashwal S, Childs N, Cranford R, Jennett B, Katz DI, et al. The minimally conscious state: definition and diagnostic criteria. Neurology. 2002;58:349–53.
62. Bruno M-A, Vanhaudenhuyse A, Thibaut A, Moonen G, Laureys S. From unresponsive wakefulness to minimally conscious PLUS and functional locked-in syndromes: recent advances in our understanding of disorders of consciousness. J Neurol. 2011;258:1373–84.
63. Products/STARSTIM - Neuroelectrics.
64. Delorme A, Makeig S. EEGLAB: an open source toolbox for analysis of single-trial EEG dynamics including independent component analysis. J Neurosci Methods. 2004;134:9–21.
65. Lehembre R, Marie-Aurélie B, Vanhaudenhuyse A, Chatelle C, Cologan V, Leclercq Y, et al. Resting-state EEG study of comatose patients: a connectivity and frequency analysis to find differences between vegetative and minimally conscious states. Funct Neurol. 2012;27:41–7.
66. Tachtsidis I, Scholkmann F. False positives and false negatives in functional near-infrared spectroscopy: issues, challenges, and the way forward. Neurophotonics. 2016;3(3):031405.
67. Scholkmann F, Kleiser S, Metz AJ, Zimmermann R, Mata Pavia J, Wolf U, et al. A review on continuous wave functional near-infrared spectroscopy and imaging instrumentation and methodology. Neuroimage. 2014;85(Pt 1):6–27.
68. Goodwin JR, Gaudet CR, Berger AJ. Short-channel functional near-infrared spectroscopy regressions improve when source-detector separation is reduced. Neurophotonics. 2014;1(1):015002.
69. Gregg NM, White BR, Zeff BW, Berger AJ, Culver JP. Brain specificity of diffuse optical imaging: improvements from superficial signal regression and tomography. Front Neuroenergetics. 2010;2:14.
70. Huppert TJ, Diamond SG, Franceschini MA, Boas DA. HomER: a review of time-series analysis methods for near-infrared spectroscopy of the brain. Appl Opt. 2009;48:D280–98.
71. Bigot J, Longcamp M, Dal Maso F, Amarantini D. A new statistical test based on the wavelet cross-spectrum to detect time-frequency dependence between non-stationary signals: application to the analysis of cortico-muscular interactions. Neuroimage. 2011;55:1504–18.
72. Encyclopedia of Bioinformatics and Computational Biology|ScienceDirect.
73. Pollonini L, Bortfeld H, Oghalai JS. PHOEBE: a method for real time mapping of optodes-scalp coupling in functional near-infrared spectroscopy. Biomed Opt Exp. 2016;7:5104–19.
74. Carnevale T, Majumdar A, Sivagnanam S, Yoshimoto K, Astakhov V, Bandrowski A, et al. The neuroscience gateway portal: high performance computing made easy. BMC Neurosci. 2014;15:P101.
75. Turgeon AF, Lauzier F, Simard J-F, Scales DC, Burns KEA, Moore L, et al. Mortality associated with withdrawal of life-sustaining therapy for

patients with severe traumatic brain injury: a Canadian multicentre cohort study. CMAJ. 2011;183:1581–8.
76. Chung DY, Claassen J, Agarwal S, Schmidt JM, Mayer SA. Assessment of noninvasive regional brain oximetry in posterior reversible encephalopathy syndrome and reversible cerebral vasoconstriction syndrome. J Intensive Care Med. 2016;31:415–9.
77. Kondziella D, Friberg CK, Wellwood I, Reiffurth C, Fabricius M, Dreier JP. Continuous EEG monitoring in aneurysmal subarachnoid hemorrhage: a systematic review. Neurocrit Care. 2015;22:450–61.
78. Zweifel C, Dias C, Smielewski P, Czosnyka M. Continuous time-domain monitoring of cerebral autoregulation in neurocritical care. Med Eng Phys. 2014;36:638–45.
79. Franceschini MA, Radhakrishnan H, Thakur K, Wu W, Ruvinskaya S, Carp S, et al. The effect of different anesthetics on neurovascular coupling. Neuroimage. 2010;51:1367–77.
80. Carpenter KLH, Young AMH, Hutchinson PJ. Advanced monitoring in traumatic brain injury: microdialysis. Curr Opin Crit Care. 2017;23:103–9.
81. Oddo M, Hutchinson PJ. Understanding and monitoring brain injury: the role of cerebral microdialysis. Intensive Care Med. 2018;44:1945–8.
82. Huschak G, Hoell T, Hohaus C, Kern C, Minkus Y, Meisel HJ. Clinical evaluation of a new multiparameter neuromonitoring device: measurement of brain tissue oxygen, brain temperature, and intracranial pressure. J Neurosurg Anesthesiol. 2009;21:155–60.
83. Sinha S, Hudgins E, Schuster J, Balu R. Unraveling the complexities of invasive multimodality neuromonitoring. Neurosurg Focus. 2017;43:E4.
84. Elmer J, Flickinger KL, Anderson MW, Koller AC, Sundermann ML, Dezfulian C, et al. Effect of neuromonitor-guided titrated care on brain tissue hypoxia after opioid overdose cardiac arrest. Resuscitation. 2018;129:121–6.
85. Lazaridis C, Robertson CS. The Role of Multimodal Invasive Monitoring in Acute Traumatic Brain Injury. Neurosurg. Clin. N. Am. W.B. Saunders; 2016. 27(4): 509–17.
86. Kempny AM, James L, Yelden K, Duport S, Farmer S, Playford ED, et al. Functional near infrared spectroscopy as a probe of brain function in people with prolonged disorders of consciousness. NeuroImage Clin. 2016;12:312–9.
87. Banville H, Gupta R, Falk TH. Mental task evaluation for hybrid NIRS–EEG brain–computer interfaces. Comput Intell Neurosci. 2017;2017:3524208. https://doi.org/10.1155/2017/3524208.
88. Shin J, Kwon J, Im C-H. A ternary hybrid EEG–NIRS brain–computer interface for the classification of brain activation patterns during mental arithmetic, motor imagery, and idle state. Front Neuroinform. 2018;12:5.
89. Iso N, Moriuchi T, Sagari A, Kitajima E, Iso F, Tanaka K, et al. Monitoring local regional hemodynamic signal changes during motor execution and motor imagery using near-infrared spectroscopy. Front Physiol. 2016;6:416.
90. Abdalmalak A, Milej D, Diop M, Shokouhi M, Naci L, Owen AM, et al. Can time-resolved NIRS provide the sensitivity to detect brain activity during motor imagery consistently? Biomed Opt Exp. 2017;8:2162.
91. Giacino JT, Kalmar K, Whyte J. The JFK Coma Recovery Scale-Revised: measurement characteristics and diagnostic utility. Arch Phys Med Rehabil. 2004;85:2020–9.
92. Almojuela A, Hasen M, Zeiler FA. The full outline of unresponsiveness (FOUR) score and its use in outcome prediction: a scoping systematic review of the adult literature. Neurocrit Care. 2019;31:162–75.
93. Foo CC, Loan JJM, Brennan PM. The relationship of the Four score to patient outcome: a systematic review. J Neurotrauma. 2019;36(17):2469–83.